Adv. Polar Upper Atmos. Res., **20**, 46–51, 2006

Research note

Field-aligned plasma motion in the converging field line geometry of anisotropic plasma pressure

Osuke Saka

Department of Physics, Kurume National College of Technology, Kurume 830-8555
E-mail: saka.o@pep.ne.jp

(Received October 19, 2005; Accepted February 22, 2006)

Abstract: In our previous report (O. Saka, Adv. Polar Upper Atmos. Res., **19**, 80, 2005), the steady-state flow characteristics in converging field line geometry has been examined by incorporating double adiabatic equations of state. In this report, we extend our previous analysis to examine how the penetration depth of plasma flow varies with a Mach number of the flow. The results obtained here suggest that the penetration depth became deeper than that of the mirror height of the single particle motion in all range of pressure anisotropy when a Mach number increased above 3.0. For a lower flow velocity, however, the flow could not penetrate below the mirror height of the single particle motion.

key words: plasma flow, converging field line geometry, anisotropic plasmas

1. Introduction

A number of works has been reported observationally and theoretically that suggest field-aligned currents as a candidate of auroral energy (*e.g.* Pashin *et al*., 1982). In addition to the field-aligned current source, there may be mechanical sources convertible to auroral energy (Sato, 1982). The sources are non-current carrying field-aligned plasma motion arising from reconnection process. In the mechanical model, plasmas are penetrated deeper toward the earth to invoke the separation of protons and electrons by mirror effect. This effect is suggested to cause electric fields that accelerate electrons for auroral energy.

MHD solutions for steady-state plasma flow in converging field geometry studied by Saka (2005) have utilized and expanded to investigate penetration depth of the plasma motions along the field lines. We applied those results to the geometries of the Earth's dipole field lines. We could show bulk characteristics of the earthward penetration of injected plasmas along the dipole field lines during substorm expansion onset.

2. Plasma flow in converging field lines

2.1. *Basic equation of the steady state field-aligned flow*

We interpreted anisotropic plasma pressures ($P_\perp \neq P_z$). Here, $\perp$ and z denote "perpendicular" and "parallel" to the field lines.

The equation that governs the field-aligned flow was given by Saka (2005). This equation was expressed as,

$$a_1 = -\frac{2\alpha_0 v_1^2}{(2\alpha_0+1)v_1^4-(2+2\alpha_0+1+v_0^2(2\alpha_0+1))v_1^2+3v_0^2}. \quad (1)$$

Here, a_1, v_0 and v_1 are cross-section normalized by the initial cross-section A_0, and flow velocities normalized by initial sound velocity C_{S0}. The velocity v_0 is an initial velocity at the start of the flow. If we can consider that the plasma sheet materials are delivered to inner magnetosphere through geosynchronous altitudes (*e.g.*, Denton *et al*., 2005), and that the flow along the Earth's dipole fields starts near geosynchronous altitudes, the parameters, A_0, C_{S0}, v_0 and α_0 (pressure anisotropy denoted by $P_{0\perp}/P_{0z}$) can be those at geosynchronous altitudes.

It is apparent that initial conditions of the flow, α_0 and v_0, determine the flow characteristics, a_1 and v_1, thereafter.

2.2. *Penetration depth of plasma flow*

An example of normalized flow velocity in the changing area of cross-section is shown in Fig. 1a for $\alpha_0=3$ and $v_0=1.4$. The flow started at $(v_1, a_1)=(1.4, 1.0)$ marked by the dot follows the arrow by slowing down the flow velocity as the area of cross-section decreases. It reaches at the point $(v_1, a_1)=(1.0, 0.65)$ marked by the

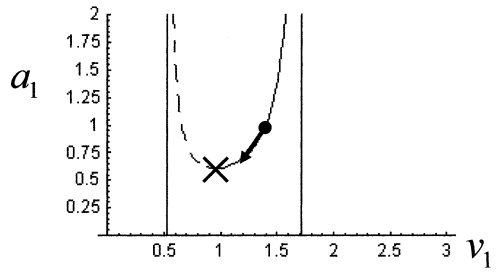

Fig. 1a. A plot of a_1 as a function of v_1. The initial conditions are $\alpha_0=3.0$ and $v_0=1.4$. The flow started along the arrow from ($a_1=1$, $v_0=1.4$), as marked by dot, with decreasing its velocity with decreasing cross-section of flux tube. The maximum penetration can be achieved at the cross. The dotted line indicates a flow in diverging fields.

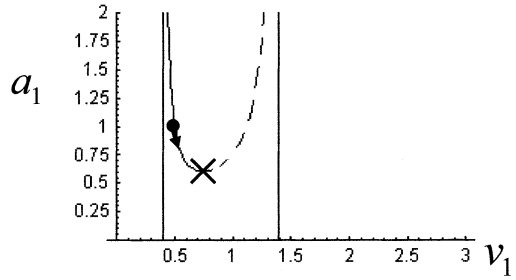

Fig. 1b. Same as Fig. 1a but initial conditions are $\alpha_0=0.7$ and $v_0=0.5$. The flow started from the dot increased its velocity with decreasing cross-section of flux tube.

cross. The area of the cross-section no longer decreases along the flow. We assume that flow reached the minimum velocity and maximum penetration of the steady-state flow. We show another example in Fig. 1b for $\alpha_0=0.7$ and $v_0=0.5$. In this case, flow started at $(v_1, a_1)=(0.5, 1.0)$ may speed up the flow velocity as the area of the cross-section decreases. It reached at the point $(v_1, a_1)=(0.78, 0.63)$ marked by the cross, where the flow shows maximum velocity and maximum penetration of the steady-state flow. The lines beyond the cross are shown by the dotted line, because the flow continues only if the field diverges.

In the first case, the flow penetrates by decelerating the velocity. In the second case, the flow penetrates by accelerating the velocity. In the text, we defined the penetration depth by "a_1". Then, the case of "no penetration" corresponds to "$a_1=1$". We note that the penetration depth and flow velocity are examined under steady-state condition. To keep the steady-state flow, the cross-section of the nozzle should be increased after passing the maximum penetration. Therefore, the penetration depth defined above does not indicate a termination of the flow. In the converging field geometry, like the Earth's dipole field lines, the steady-state flow might be inapplicable beyond that depth. It is conceivable, however, that the flows eventually stop and reflected back forming diverging flow along the dipole field lines. In this report, however, we do not discuss the diverging flow. In addition, there appeared solutions with negative a_1 beside the line plotted in Fig. 1a and 1b. Those negative solutions do not cover the initial condition, $a_1=1$.

The flows keep acceleration or deceleration in the converging field geometries, once they are initially accelerated or decelerated. In addition, the initial conditions regarding acceleration/deceleration can be uniquely determined by the parameters α_0 and v_0. In Fig. 2, we show in α_0–v_0 plane the flow characteristics in terms of acceleration or deceleration. The line that separates those two regions is referred to as the "critical velocity". The critical velocity line corresponds to the line connecting crosses in Fig. 1. Flows are initially accelerated/decelerated below/above the critical velocity. The flow penetrates some distance thereafter. A distribution of penetration depth is shown in Fig. 3 in the same α_0–v_0 plane. Note that no penetration takes place along the line of the critical velocity. A deeper penetration can be seen in the flow above the critical velocity. In below, we will compare the penetration depth with the mirror height of single particle approximation. Figure 4a demonstrates penetration depth of the flow as

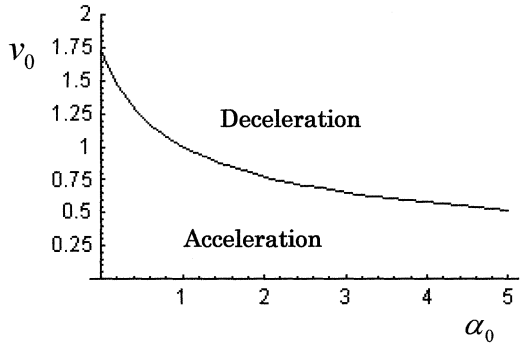

Fig. 2. A line of critical velocity in α_0–v_0 plane. Flows above the critical velocity are decelerated. Flows below the critical velocity are accelerated.

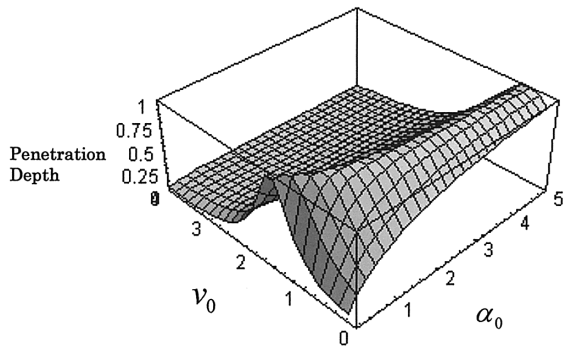

Fig. 3. A 3-D illustration of penetration depth in α_0–v_0 plane. Penetration depth is deep as the number of the vertical axis decreases. Because of an unstable numerical calculation, $\alpha_0 \geq 0.1$ is plotted.

a function of α_0 for the condition $v_0=0.1$. In the figure, the mirror height estimated by the single particle motion is plotted for reference. The mirror height can be written as

$$a_1=\frac{\alpha_0}{1.0+\alpha_0},$$

where we assumed

$$\left(\frac{V_{0\perp}}{V_{0z}}\right)^2=\frac{P_{0\perp}}{P_{0z}}.$$

In the limit of $v_0=0$, the penetration depth could be given as

$$a_1=\frac{\alpha_0}{1.5+\alpha_0}.$$

In Fig. 4b, penetration depth of the flow for the case of $v_0=1.0$ is shown. The penetration depth is shallower than the mirror height of the single particle motion in the range below $\alpha_0 \approx 4.5$. A deep penetration can be seen only at a small pressure anisotropy condition. When v_0 increased above 3.0, the penetration depth became deeper than that of the mirror height of the single particle motion in all range of α_0, as can be seen in Fig. 4c. It is conceivable that the increasing fluid velocities at the initial point give the increasing velocity offset toward the field lines in velocity space. High velocity along the field lines may cause field-aligned pitch angle distribution of particles. In low velocities, the pitch angle distribution shows less velocity offset toward the field lines. Once those distributions were averaged over the velocity space, a change of penetration depth as a function of initial velocities could be expected as described above.

Finally, it is worthy to note a change of pressure anisotropy during the fluid penetration. Because change of pressure anisotropy can be written as,

$$\alpha_1-\alpha_0=\alpha_0\left(\frac{v_1^2}{v_0^2}\cdot\frac{1}{a_1}-1\right),$$

it is apparent that pressure anisotropy increases in the acceleration region, and decreases

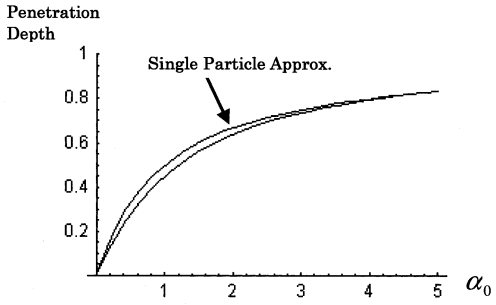

Fig. 4a. A penetration depth for $v_0=0.1$ as a function of pressure anisotropy α_0. The mirror height of single particle motion is plotted for reference.

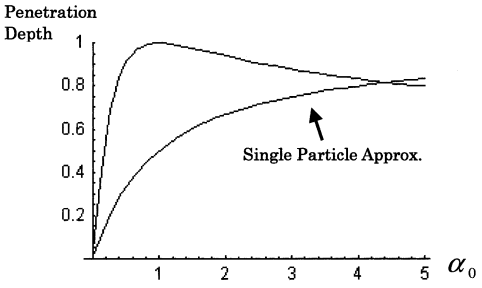

Fig. 4b. Same as Fig. 4a but for $v_0=1.0$.

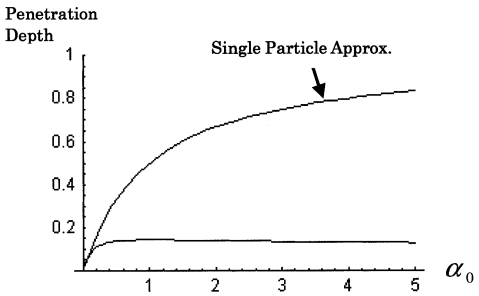

Fig. 4c. Same as Fig. 4a but for $v_0=3.0$

in deceleration region. However, pressure anisotropy increased again in deceleration region when initial velocities increased further, because decrease of v_1 becomes slow as compared with that of a_1. For initially isotropic pressure, the anisotropy at the maximum penetration depth increased to 5.5 for $v_0=0.33$, decreased to 0.9 for $v_0=1.4$, and increased again to 2.3 for $v_0=3.0$.

3. Summary

It has been suggested that plasma sheet materials transported by the earthward fast flow from the midtail plasma sheet (Sergeev *et al*., 1996; Nakamura *et al*., 2001) may intrude from geosynchronous altitudes into the inner magnetosphere (*e.g.* Denton *et al*., 2005). It is conceivable that earthward flow of the plasma sheet material along the dipole field lines may originate from geosynchronous altitudes. The sound velocity of plasmas at geosynchronous altitudes can be estimated to be 9.7×10^2 km/s, if major contributions are from ions (T_i~10 keV, *e.g.* Birn *et al*., 1997). We assume that field-aligned flow velocity V_0 could be determined by local Alfvén velocity (*e.g.* Sato, 1982). The local Alfvén velocity at geosynchronous altitudes might be estimated to be 2.2×10^3 km/s by substituting the parameters, 10^0 cm^{-3} of ion density (Birn *et al*., 1997)

and 100 nT of field magnitudes. Those parameters lead to ~2.2 of local Mach number at geosynchronous altitudes. If we can utilize those calculations, the estimated penetration depth could be 0.5 for pressure anisotropies above 1.0. Then, the estimated penetration depth corresponds to the flux tube cross-sections at about 50% of the initial cross-section. In the dipole field geometry, the flows departed from geosynchronous orbit ($7R_e$) would penetrate along the field lines down to the altitudes of $4.8R_e$ (31000 km). The penetration altitudes lowered to $3.6R_e$ (27000 km) if the Mach number at geosynchronous altitudes increased to 3.0. Those bulk characteristics of the penetration can be discussed in our future work, in conjunction with the non-current carrying field-aligned plasma motion proposed by Sato (1982).

Acknowledgments

The editor thanks anonymous referees for their help in evaluating this paper.

References

Birn, J., Thomsen, M.F., Borovsky, J.E., Reeves, G.D., McComas, D.J. and Belian, R.D. (1997): Characteristic plasma properties during dispersionless substorm injections at geosynchronous orbit. J. Geophys. Res., **102**, 2309–2324.

Denton, M.H., Thomsen, M.F., Korth, H., Lynch, S., Zhang, J.C. and Liemohn, M.W. (2005): Bulk plasma properties at geosynchronous orbit. J. Geophys. Res., **110**, A07223, doi: 10.1029/2004JA010861.

Nakamura, R., Baumjohann, W., Brittnacher, M., Sergeev, V.A., Kubyshkina, M., Mukai, T. and Liou, K. (2001): Flow bursts and auroral activations: Onset timing and foot point location. J. Geophys. Res., **106**, 10777–10789.

Pashin, A.B., Glasmeier, K.H., Baumjohann, W., Raspopov, O.M., Yahnin, A.G., Opgenoorth, H.J. and Pellinen, R.J. (1982): Pi2 magnetic pulsations. Auroral break-ups, and the substorm current wedge: A case study. J. Geophys., **51**, 223–233.

Saka, O. (2005): Plasma flow characteristics in converging field line geometry in anisotropic plasmas. Adv. Polar Upper Atmos. Res., **19**, 80–83.

Sato, T. (1982): Auroral physics. Magnetospheric Plasma Physics, ed. by A. Nishida. Tokyo, D. Reidel, 197–243.

Sergeev, V.A., Angelopoulos, V., Gosling, J.T., Cattel, C.A. and Russel, C.T. (1996): Detection of localized, plasma-depleted flux tubes of bubbles in the midtail plasma sheet. J. Geophys. Res., **101**, 10817–10826.